

# GOSUS: Grassmannian Online Subspace Updates with Structured-sparsity

## Supplement Material

Anonymous ICCV submission

Paper ID 342

### 1. Detailed analysis of technical results in the main paper

This section includes additional details of a few observations and theorems summarized in the main paper.

#### 1.1. The matrix in the linear system has a special structure

**Observation 1.** For  $\lambda > 0, U^{*T}U^* = I_d, \rho_i > 0, \forall i \in \{1, \dots, l\}$ , we have  $A \succ 0$ .

*Proof.* Observe that  $A$  is given by,

$$A \leftarrow \begin{bmatrix} \lambda I_d & \lambda U^{*T} \\ \lambda U^* & \lambda I_n + \sum_{i=1}^l \rho_i D^i \end{bmatrix} \quad (1)$$

and denoting  $Q = \sum_{i=1}^l \rho_i D^i$ , we have (for any  $(\mathbf{w}, \mathbf{x})$ ),

$$\begin{aligned} \begin{bmatrix} \mathbf{w} \\ \mathbf{x} \end{bmatrix}^T A \begin{bmatrix} \mathbf{w} \\ \mathbf{x} \end{bmatrix} &= [\lambda(\mathbf{w}^T + \mathbf{x}^T U^*) \quad \lambda(\mathbf{w}^T U^{*T} + \mathbf{x}^T) + \mathbf{x}^T Q] \begin{bmatrix} \mathbf{w} \\ \mathbf{x} \end{bmatrix} \\ &= \lambda(\mathbf{w}^T \mathbf{w} + \mathbf{x}^T U^* \mathbf{w} + \mathbf{w}^T U^{*T} \mathbf{x} + \mathbf{x}^T \mathbf{x}) + \mathbf{x}^T Q \mathbf{x} \\ &= \lambda \|\mathbf{x} + U^* \mathbf{w}\|_2^2 + \mathbf{x}^T Q \mathbf{x} \end{aligned} \quad (2)$$

Let us check both terms in (2). Observe that  $\forall \mathbf{x}, \mathbf{x}^T Q \mathbf{x} \geq 0$ . Next, as  $\lambda \|\mathbf{x} + U^* \mathbf{w}\|_2^2 \geq 0$ , for the LHS of the identity in (2), we have

$$\begin{bmatrix} \mathbf{w} \\ \mathbf{x} \end{bmatrix}^T A \begin{bmatrix} \mathbf{w} \\ \mathbf{x} \end{bmatrix} \geq 0 \quad (3)$$

For the equality to hold in (3), we need to have both the terms,  $\|\mathbf{x} + U^* \mathbf{w}\|_2^2$  and  $\mathbf{x}^T Q \mathbf{x}$  equal to 0. But  $Q \succ 0$  because  $\mathbf{x}^T Q \mathbf{x} = 0$  only when  $\mathbf{x} = 0$ . Further,  $\mathbf{w} = 0$  whenever  $\mathbf{x} = 0$ , for  $\|\mathbf{x} + U^* \mathbf{w}\|_2^2$  to be zero. Hence equality in (3) holds only when  $\mathbf{w}$  and  $\mathbf{x}$  are zero.  $\square$

#### 1.2. Convergence properties

**Theorem 1.** For  $\lambda > 0, \mu_i > 0, \rho_i > 0, \forall i \in \{1, \dots, l\}$ , the sequence  $\{(\mathbf{w}_k, \mathbf{x}_k, \{\mathbf{z}_k^i\}, \{\mathbf{y}^i\})\}$  generated by Alg. 1 from any initial point  $(\mathbf{w}_0, \mathbf{x}_0, \{\mathbf{z}_0^i\}, \{\mathbf{y}_0^i\})$  converges to  $(\mathbf{w}^*, \mathbf{x}^*, \{\mathbf{z}^{i*}\}, \{\mathbf{y}^{i*}\})$ , which minimizes  $\mathcal{L}$  at fixed  $U^*$ .

*Proof.* Our proof emulates the convergence proof in [2]. We first show that model with a fixed  $U$  agrees with the standard ADMM formulation in [2].

$$\begin{aligned} \min_{\mathbf{w}, \mathbf{x}, \mathbf{z}^i} \quad & \sum_{i=1}^l \mu_i \|\mathbf{z}^i\|_2 + \frac{\lambda}{2} \|U\mathbf{w} + \mathbf{x} - \mathbf{v}\|_2^2 \\ \text{s.t.} \quad & \mathbf{z}^i = D^i \mathbf{x}, \end{aligned} \quad (4)$$

If we denote  $f(\mathbf{w}, \mathbf{x}) = \frac{\lambda}{2} \|U\mathbf{w} + \mathbf{x} - \mathbf{v}\|_2^2, g(\{\mathbf{z}^i\}) = \sum_{i=1}^l \mu_i \|\mathbf{z}^i\|_2$ , our problem (4) is really a special case of (3.1) in [2].

We next need to show that (4) satisfies the two main assumptions made in the convergence proof given in [2].

**Assumption (i)**  $f(\mathbf{w}, \mathbf{x})$  and  $g(\{\mathbf{z}^i\})$  are both convex, proper and closed.

**Assumption (ii)**  $\mathcal{L}(\mathbf{w}^*, \mathbf{x}^*, \{\mathbf{z}^{i*}\}, \{\mathbf{y}^{i*}\})$  has a saddle point.

For notational simplicity, denote  $\mathbf{c} = [\mathbf{w} \ \mathbf{x}]^T$ ,  $\hat{U} = [U \ I_n]$  and  $\hat{D}^i = [0_{n \times d} \ D^i]$  ( $0_{n \times d}$  is a  $n \times d$  zero matrix). Using this notation,  $f(\mathbf{w}, \mathbf{x}) = f(\mathbf{c}) = \frac{\lambda}{2} \|\hat{U}\mathbf{c} - \mathbf{v}\|_2^2$ . Here,  $f(\mathbf{c})$  is convex. By non-negativity of the norm squared function,  $f(\mathbf{c}) \geq 0 > -\infty$ , and taking  $\mathbf{c} = 0$ , we have  $f(\mathbf{c}) = \|\mathbf{v}\|_2^2 < \infty$ . Hence,  $f(\mathbf{c})$  is proper. Further, the domain of  $\mathbf{c}$  is  $\mathcal{R}^{n+d}$  and  $f(\mathbf{c})$  is continuous on that domain. Following the closure property of proper convex functions [3], we see that  $f(\mathbf{c})$  is closed.

Following similar arguments as above, consider  $g_1(\mathbf{z}^i) = \|\mathbf{z}^i\|_2$ . Since  $\|\cdot\|_2$  is convex and increasing and as  $\mathbf{z}^i = D^i x$ , using the composition rule,  $g_1(\mathbf{z}^i)$  is convex. Using the non-negativity of the norm and by taking  $\mathbf{x} = 0$  which gives  $g_1(\mathbf{z}^i) < \infty$ , we have  $g_1(\mathbf{z}^i)$  is proper. Finally, observe that  $g_1(\mathbf{z}^i)$  is a continuous function of  $\mathbf{x}$ , and the domain on  $\mathbf{x}$  ( $\mathcal{R}^n$ ) is closed. Hence,  $g_1(\mathbf{z}^i)$  a closed proper convex function. The non-negative sum of closed proper convex functions is also closed proper convex when the domain of summation remains unchanged. This concludes the proof of the first assumption.

For the second part, using the new notation, the augmented Lagrangian is,

$$\mathcal{L}_0(\mathbf{w}, \mathbf{x}, \{\mathbf{z}^i\}, \{\mathbf{y}^i\}) \sim \mathcal{L}_0(\mathbf{c}, \{\mathbf{z}^i\}, \{\mathbf{y}^i\}) = \sum_{i=1}^l \mu_i \|\mathbf{z}^i\|_2 + \frac{\lambda}{2} \|\hat{U}\mathbf{c} - \mathbf{v}\|_2^2 + \sum_{i=1}^l \mathbf{y}^{iT} (\mathbf{z}^i - \hat{D}^i \mathbf{c}) \quad (5)$$

First, observe that the domain of  $\mathbf{c}$ ,  $\mathbf{z}^i$ , and  $\mathbf{y}^i$  is  $\mathcal{R}^{n+d}$ ,  $\mathcal{R}^n$ , and  $\mathcal{R}_+^n$  respectively, which are compact and convex sets. Fixing  $\mathbf{y}^i$ 's for  $i = 1, \dots, l$ ,  $\mathcal{L}_0$  is a convex function of  $\mathbf{c}$  and  $\mathbf{z}^i$ . This follows from the fact that the first two terms in (5) are convex and the last term is affine in the primal parameters (when  $\mathbf{y}^i$ 's are fixed). So, there exists a triple,  $(\mathbf{c}^*, \{\mathbf{z}^{i*}\}, \{\mathbf{y}^{i*}\})$  such that

$$\mathcal{L}_0(\mathbf{c}^*, \{\mathbf{z}^{i*}\}, \{\mathbf{y}^{i*}\}) \leq \mathcal{L}_0(\mathbf{c}, \{\mathbf{z}^i\}, \{\mathbf{y}^i\}).$$

Further, for a fixed  $(\mathbf{c}, \mathbf{z}^i)$ ,  $\mathcal{L}_0$  is an linear combination of affine functions in  $\mathbf{y}^i$ 's. Hence it is concave. So, there exists a triple,  $(\mathbf{c}^*, \{\mathbf{z}^{i*}\}, \{\mathbf{y}^{i*}\})$

$$\mathcal{L}_0(\mathbf{c}^*, \{\mathbf{z}^{i*}\}, \{\mathbf{y}^i\}) \leq \mathcal{L}_0(\mathbf{c}^*, \{\mathbf{z}^{i*}\}, \{\mathbf{y}^{i*}\}).$$

Thus,  $\mathcal{L}_0$  has a saddle point  $(\mathbf{c}^*, \{\mathbf{z}^{i*}\}, \{\mathbf{y}^{i*}\})$  in the primal–dual domain. □

### 1.3. The updating scheme for $U$ : Part one

$$U(\eta) = U + (\cos(\sigma\eta) - 1)U\mathbf{q}\mathbf{q}^T - \sin(\sigma\eta)\mathbf{p}\mathbf{q}^T \quad (13)$$

Recall the compact SVD of  $\nabla\mathcal{L}$  by (12) in the main paper ( $\mathcal{L}$  is the Lagrangian),

$$\nabla\mathcal{L} = \frac{\mathbf{s}}{\|\mathbf{s}\|} \times \|\mathbf{s}\| \|\mathbf{w}^*\| \times \left( \frac{\mathbf{w}^*}{\|\mathbf{w}^*\|} \right)^T = \mathbf{p}\sigma\mathbf{q}^T$$

Here, we approximate the full SVD with

$$\nabla\mathcal{L} = S\Sigma V^T = [\mathbf{p}_1 \ \mathbf{p}_2 \ \cdots \ \mathbf{p}_d] \times \text{diag}(\sigma, 0, \dots, 0) \times [\mathbf{q}_1 \ \mathbf{q}_2 \ \cdots \ \mathbf{q}_d]^T$$

where  $S = [\mathbf{p}_1 \ \mathbf{p}_2 \ \cdots \ \mathbf{p}_d]$ ,  $\Sigma = \text{diag}(\sigma, 0, \dots, 0)$ ,  $V = [\mathbf{q}_1 \ \mathbf{q}_2 \ \cdots \ \mathbf{q}_d]$ ,  $\mathbf{p}_2, \dots, \mathbf{p}_d$  and  $\mathbf{q}_2, \dots, \mathbf{q}_d$  are slack orthonormal basis, which will be omitted by the zero singular values.

By Thm. 2.65 in [1], we can update our subspace  $U$  with stepsize  $\eta$  by

$$U(\eta) = [UV \ -S] \begin{bmatrix} \cos(\Sigma\eta) \\ \sin(\Sigma\eta) \end{bmatrix} V^T$$

Observe that the above update involves full matrix operations. It can be simplified as,

$$\begin{aligned}
 U(\eta) &= UV \cos(\Sigma\eta)V^T - S \sin(\Sigma\eta)V^T \\
 &= UV \cos(\text{diag}(\sigma\eta, 0, \dots, 0))V^T - S \sin(\text{diag}(\sigma\eta, 0, \dots, 0))V^T \\
 &= UV \text{diag}(\cos(\sigma\eta), 1, \dots, 1)V^T - S \text{diag}(\sin(\sigma\eta), 0, \dots, 0)V^T \\
 &= UV \text{diag}(1, 1, 1, \dots, 1)V^T + UV \text{diag}(\cos(\sigma\eta) - 1, 0, \dots, 0)V^T - S \text{diag}(\sin(\sigma\eta), 0, \dots, 0)V^T \\
 &= UV I_d V^T + UV \text{diag}(\cos(\sigma\eta) - 1, 0, \dots, 0)V^T - S \text{diag}(\sin(\sigma\eta), 0, \dots, 0)V^T \\
 &= U + (\cos(\sigma\eta) - 1)U \mathbf{q}\mathbf{q}^T - \sin(\sigma\eta)\mathbf{p}\mathbf{q}^T
 \end{aligned}$$

The last identity is what appears in the main paper.

#### 1.4. The updating scheme for $U$ : Part two

**Lemma 1.** *The subspace updating procedure (13) preserves the column-wise orthogonality of  $U$ .*

*Proof.* The residual vector  $\mathbf{s}$  is orthogonal to all the columns of  $U$ , thus we have

$$U^T \mathbf{p} = U^T \frac{\mathbf{s}}{\|\mathbf{s}\|} = 0$$

Also,  $\mathbf{p}, \mathbf{q}$  are unary vectors, hence  $\mathbf{q}^T \mathbf{q} = 1, \mathbf{p}^T \mathbf{p} = 1$ . Now we show  $U(\eta)^T U(\eta) = I_d$ :

$$\begin{aligned}
 U(\eta)^T U(\eta) &= (U + (\cos(\sigma\eta) - 1)U \mathbf{q}\mathbf{q}^T - \sin(\sigma\eta)\mathbf{p}\mathbf{q}^T)^T (U + (\cos(\sigma\eta) - 1)U \mathbf{q}\mathbf{q}^T - \sin(\sigma\eta)\mathbf{p}\mathbf{q}^T) \\
 &= U^T U + (\cos(\sigma\eta) - 1)U^T U \mathbf{q}\mathbf{q}^T - \sin(\sigma\eta)U^T \mathbf{p}\mathbf{q}^T + (\cos(\sigma\eta) - 1)\mathbf{q}\mathbf{q}^T U^T U \\
 &\quad + (\cos(\sigma\eta) - 1)^2 \mathbf{q}\mathbf{q}^T U^T U \mathbf{q}\mathbf{q}^T - (\cos(\sigma\eta) - 1) \sin(\sigma\eta) \mathbf{q}\mathbf{q}^T U^T \mathbf{p}\mathbf{q}^T \\
 &\quad - \sin(\sigma\eta) \mathbf{q}\mathbf{p}^T U - (\cos(\sigma\eta) - 1) \sin(\sigma\eta) \mathbf{q}\mathbf{p}^T U \mathbf{q}\mathbf{q}^T + \sin^2(\sigma\eta) \mathbf{q}\mathbf{p}^T \mathbf{p}\mathbf{q}^T \\
 &= I_d + (\cos(\sigma\eta) - 1)\mathbf{q}\mathbf{q}^T - 0 + (\cos(\sigma\eta) - 1)\mathbf{q}\mathbf{q}^T + (\cos(\sigma\eta) - 1)^2 \mathbf{q}\mathbf{q}^T \\
 &\quad - 0 - 0 - 0 + \sin^2(\sigma\eta)\mathbf{q}\mathbf{q}^T \\
 &= I_d + (2 \cos(\sigma\eta) - 2 + \cos^2(\sigma\eta) - 2 \cos(\sigma\eta) + 1 + \sin^2(\sigma\eta))\mathbf{q}\mathbf{q}^T \\
 &\quad (2 \cos(\sigma\eta) \text{ cancels out and } \cos^2(\sigma\eta) + \sin^2(\sigma\eta) = 1) \\
 &= I_d
 \end{aligned}$$

Thus, the subspace updating procedure preserves the column-wise orthogonality of  $U$ . □

## 2. More Details on Experiments

In the main paper, we presented representative ROC curves for 6 video datasets. Figs. 1 and Fig. 2 give the ROC curves for all 12 videos. Observe that the ROCs in Fig. 2 are zoomed in versions of those in Fig. 1.

## References

- [1] T. Arias, A. Edelman, and S. Smith. The geometry of algorithms with orthogonality constraints. *SIAM Journal on Matrix Analysis and Applications*, 20:303–353, 1998. 2
- [2] S. Boyd, N. Parikh, E. Chu, B. Peleato, and J. Eckstein. Distributed optimization and statistical learning via the alternating direction method of multipliers. *Foundations and Trends in Machine Learning*, 3(1):1–122, 2011. 1
- [3] R. T. Rockafellar. *Convex Analysis*. Princeton, NJ: Princeton University Press, 1970. 2

324  
325  
326  
327  
328  
329  
330  
331  
332  
333  
334  
335  
336  
337  
338  
339  
340  
341  
342  
343  
344  
345  
346  
347  
348  
349  
350  
351  
352  
353  
354  
355  
356  
357  
358  
359  
360  
361  
362  
363  
364  
365  
366  
367  
368  
369  
370  
371  
372  
373  
374  
375  
376  
377

378  
379  
380  
381  
382  
383  
384  
385  
386  
387  
388  
389  
390  
391  
392  
393  
394  
395  
396  
397  
398  
399  
400  
401  
402  
403  
404  
405  
406  
407  
408  
409  
410  
411  
412  
413  
414  
415  
416  
417  
418  
419  
420  
421  
422  
423  
424  
425  
426  
427  
428  
429  
430  
431

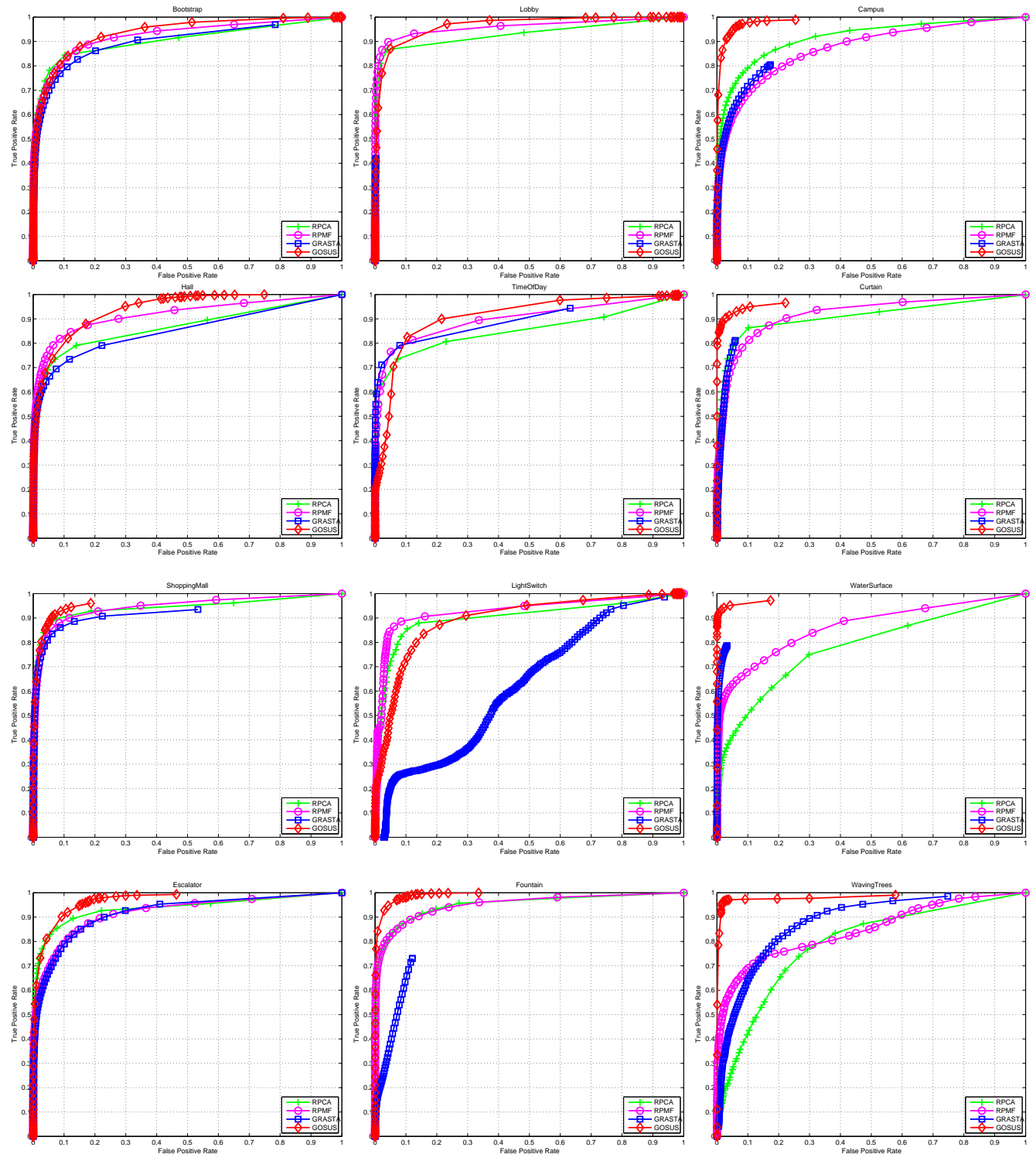


Figure 1: ROC curves of 12 datasets for three different dataset categories showing the performance of RPCA, RPFM, GRASTA and GOSUS.

432  
433  
434  
435  
436  
437  
438  
439  
440  
441  
442  
443  
444  
445  
446  
447  
448  
449  
450  
451  
452  
453  
454  
455  
456  
457  
458  
459  
460  
461  
462  
463  
464  
465  
466  
467  
468  
469  
470  
471  
472  
473  
474  
475  
476  
477  
478  
479  
480  
481  
482  
483  
484  
485

486  
487  
488  
489  
490  
491  
492  
493  
494  
495  
496  
497  
498  
499  
500  
501  
502  
503  
504  
505  
506  
507  
508  
509  
510  
511  
512  
513  
514  
515  
516  
517  
518  
519  
520  
521  
522  
523  
524  
525  
526  
527  
528  
529  
530  
531  
532  
533  
534  
535  
536  
537  
538  
539

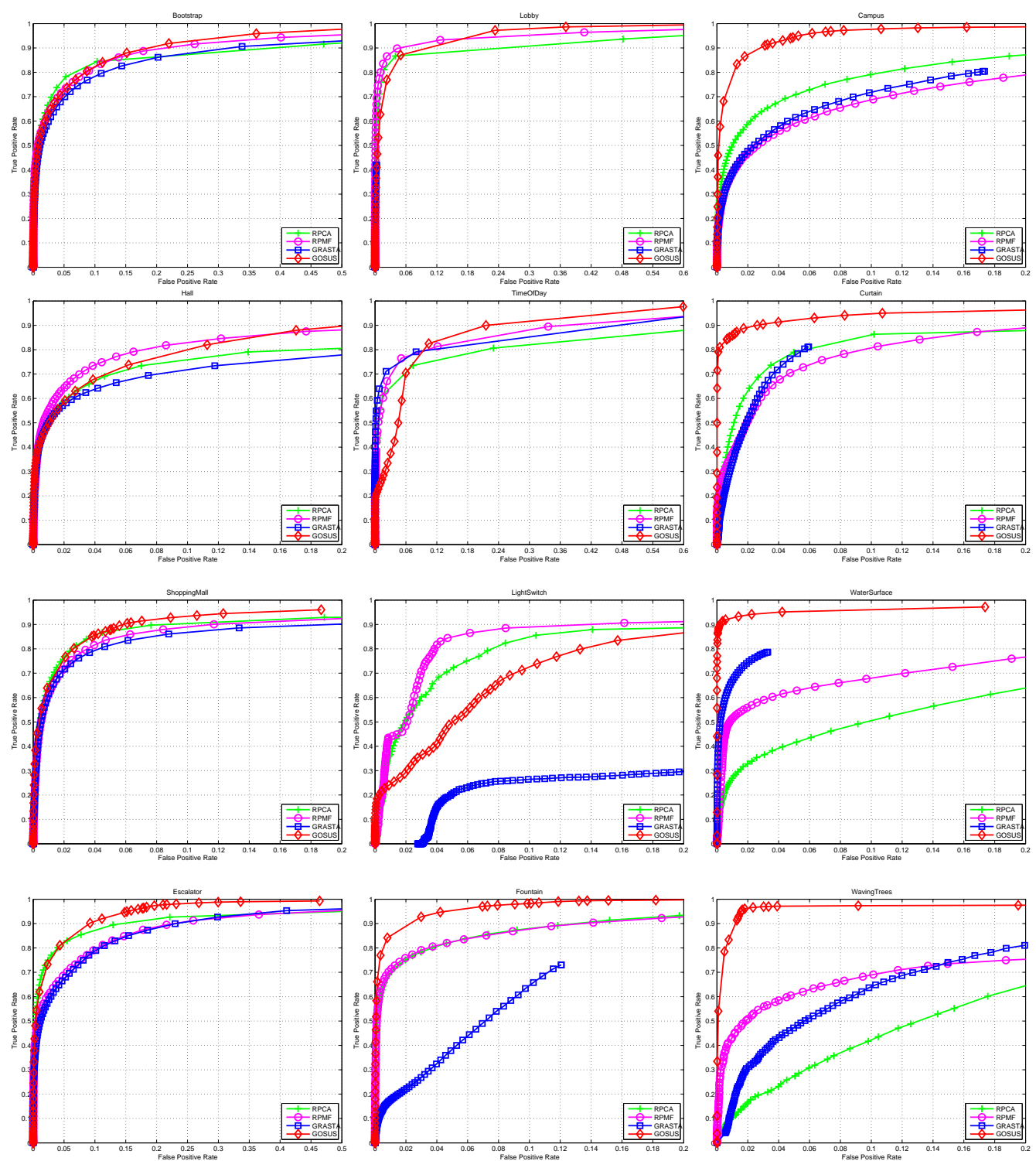


Figure 2: Zoomed in (adjusted false positive rate range) ROC curves of 12 datasets for three different dataset categories showing the performance of RPCA, RPFM, GRASTA and GOSUS.